Brain, Behavior, and Immunity 134 (2026) 106463

Contents lists available at ScienceDirect

Brain Behavior and Immunity

journal homepage: www.elsevier.com/locate/ybrbi

Full-length Article

Prenatal-lactational alcohol exposure induces sex-specific CX_3CL1/CX_3CR1 dysregulation linked to neuroendocrine imbalance and cardiovascular risk☆

Dina Medina-Vera [a,b,c,d], Alba García-Baos [e], Mireia Medrano [e], Laura Martín-Chaves [a,b,f], Jorge Rodríguez-Capitán [a,d,f], Fernando Rodríguez de Fonseca [a,g], Antonia Serrano [a,h], Manuel Jiménez-Navarro [a,b,d,f], Olga Valverde [e,*], Francisco Javier Pavón-Morón [a,b,d,f,**]

[a] Instituto de Investigación Biomédica de Málaga y Plataforma en Nanomedicina - IBIMA Plataforma BIONAND, 29590 Málaga, Spain
[b] Facultad de Medicina, Universidad de Málaga 29010 Málaga, Spain
[c] Department of Neurobiology, Care Sciences and Society (NVS), Karolinska Institutet, 17177 Solna, Sweden
[d] Unidad Clínica de Cardiología y Cirugía Cardiovascular, Hospital Universitario Virgen de la Victoria, 29010 Málaga, Spain
[e] Neurobiology of Behavior Research Group (GReNeC-NeuroBio), Department of Medicine and Life Sciences (MELIS), Universitat Pompeu Fabra, 08003 Barcelona, Spain
[f] Centro de Investigación Biomédica en Red Enfermedades Cardiovasculares (CIBERCV), Instituto de Salud Carlos III, 28029 Madrid, Spain
[g] Unidad de Gestión Clínica de Neurología, Hospital Regional Universitario de Málaga 29010 Málaga, Spain
[h] Unidad de Gestión Clínica de Salud Mental, Hospital Regional Universitario de Málaga 29010 Málaga, Spain

ARTICLE INFO

Keywords:
Anxiety-like behavior
Cardiovascular risk
FASD
Fractalkine
Inflammation
PLEA
Sex differences
Stress

ABSTRACT

Fetal alcohol spectrum disorder is associated with lasting neurodevelopmental and cardiovascular dysfunctions. The fractalkine axis CX_3CL1/CX_3CR1, a chemokine and its sole known receptor expressed in microglia and myeloid/endothelial cells, coordinates neuroimmune and vascular responses. We tested whether prenatal-lactational alcohol exposure (PLAE) is associated with sex-specific dysregulation of this axis along with integrated behavioral, neuroendocrine, inflammatory, and cardiovascular signatures.

Pregnant C57BL/6 dams consumed 20% ethanol using a drinking-in-the-dark (DID) paradigm throughout gestation and lactation. Adult offspring (PND60–70) underwent behavioral testing (elevated plus maze and tail suspension test); plasma profiling of corticosterone, cytokines/chemokines, endothelial/coagulation markers, and matrix-remodeling enzymes; and cardiac transcriptional assays for stress- and inflammation-related genes (including *Cx3cr1*). Analyses were stratified by sex.

PLAE females exhibited increased anxiety-like behavior, two-fold higher plasma CX_3CL1, and upregulated cardiac *Cx3cr1* compared with control females. PLAE males showed no behavioral or endocrine changes but evidence of matrix remodeling (elevated proMMP-9, reduced sP-Selectin). Across sexes, PLAE was associated with a proinflammatory/endothelial-activation profile (elevated IL13, IL18, and PAI-1, reduced CXCL16, higher proMMP-9) and altered cardiac expression of *Nr3c2*, *Tnfrsf1a*, *Tlr4*, and *Nfkbia*, compatible with early vascular risk. Independent of exposure, females exhibited reduced immobility and higher corticosterone, IL5, IL13, sE-Selectin, and thrombomodulin. Plasma CX_3CL1 correlated inversely with exploratory and stress-coping behaviors, and positively with corticosterone, inflammatory/vascular markers, and cardiac *Cx3cr1* and *Tnfrsf1a*.

PLAE is associated with sex-specific dysregulation of the CX_3CL1/CX_3CR1 axis and convergent neuroimmune-vascular signatures indicative of subclinical endothelial dysfunction. These associative findings support the hypothesis that fractalkine-pathway modulation may mitigate long-term neurobehavioral and cardiovascular vulnerability after PLAE, warranting causal testing.

☆ This article is part of a special issue entitled: 'Brain-immune-heart connections' published in Brain Behavior and Immunity.

* Corresponding author at: Universitat Pompeu Fabra, Dr. Aiguader 88, 08003 Barcelona, Spain.
** Corresponding author at: IBIMA Plataforma BIONAND, Severo Ochoa 35, 29590 Málaga, Spain.
E-mail addresses: olga.valverde@upf.edu (O. Valverde), javier.pavon@ibima.eu (F.J. Pavón-Morón).

https://doi.org/10.1016/j.bbi.2026.106463
Received 15 July 2025; Received in revised form 12 January 2026; Accepted 25 January 2026
Available online 26 January 2026

1. Introduction

Alcohol is the most widely consumed psychoactive substance globally, and its chronic use can lead to alcohol use disorder (AUD), a complex condition involving psychological and physiological factors (MacKillop et al., 2022). AUD is often accompanied by psychiatric comorbidities such as depression and anxiety (Rudenstine et al., 2020; Howe et al., 2021), and is associated with cognitive impairments affecting memory, attention, and flexibility (Liu et al., 2024). Although traditionally more common in men, recent data from Spain show that alcohol use among adolescent girls has surpassed that of boys since the late 20th century, highlighting the importance of incorporating a gender perspective in national addiction strategies (Smith et al., 2021; Park and Kim, 2020).

Alcohol consumption during pregnancy is particularly harmful, with potentially severe consequences for fetal development (Oei, 2020). Maternal alcohol intake can result in a spectrum of persistent morphological, behavioral, cardiovascular, and neurodevelopmental impairments collectively termed fetal alcohol spectrum disorders (FASD) (Almeida et al., 2020). Among the manifestations of FASD, fetal alcohol syndrome, characterized by central nervous system damage (Bariselli and Lovinger, 2021), facial dysmorphology (Yang et al., 2012), and motor coordination deficits (Cantacorps et al., 2017), is the most severe outcome of prenatal and lactational alcohol exposure (PLAE) (Gupta et al., 2016).

The neurological and developmental consequences of FASD are well documented; however, emerging clinical and preclinical studies indicate that developmental alcohol also disrupts cardiovascular regulation and vascular health. These effects include early autonomic dysregulation, altered heart-rate variability, endothelial dysfunction, and extracellular matrix remodeling (Atum et al., 2023; Ninh et al., 2019; Jurczyk et al., 2024). Such changes may precede overt cardiovascular disease and suggest that PLAE programs long-term cardiovascular vulnerability from early stages of life.

In parallel with these peripheral alterations, accumulating evidence implicates neuroimmune dysregulation as a central mechanism underlying FASD. Prenatal and early postnatal alcohol exposure has been shown to induce persistent microglial activation, exaggerated inflammatory signaling, and altered neuroimmune communication (Cantacorps et al., 2017; Bake et al., 2021). These processes are believed to contribute not only to behavioral dysfunction but also to peripheral inflammatory alterations that impact vascular integrity.

Certain biological systems are highly susceptible to disruptions caused by stress, inflammation, and external factors such as alcohol consumption (Libby, 2021; Henein et al., 2022). CX_3CL1 (fractalkine) is a chemokine with dual roles in inflammation and homeostasis. It is constitutively expressed primarily by neurons and is inducible in vascular endothelium and smooth-muscle cells under inflammatory conditions (Paolicelli et al., 2014; Umehara et al., 2001). Its cognate (and sole known) receptor, CX_3CR1, is highly expressed by microglia in the central nervous system (CNS) and by peripheral myeloid populations (e.g., monocytes/macrophages and dendritic cells), as well as subsets of NK and T lymphocytes (Paolicelli et al., 2014; Umehara et al., 2001; Sallusto et al., 2000). This chemokine pathway plays a critical role in the CNS by regulating neuroplasticity, synaptic pruning, and microglial activation (Arnoux and Audinat, 2015). Recent studies show that CX_3CL1/CX_3CR1 signaling regulates neuroendocrine responses and stress-coping behaviors, and that this pathway can be modified by early alcohol exposure and stress (Medina-Vera et al., 2025; Momin et al., 2023). Notably, the CX_3CL1/CX_3CR1 axis is not restricted to the CNS; it is also implicated in atherosclerosis, vascular inflammation, and endothelial dysfunction, all key contributors to cardiovascular disease (Apostolakis and Spandidos, 2013).

Despite extensive research on the neurological and developmental sequelae of FASD, relatively little is known about its cardiovascular effects. The convergence of neuroimmune and vascular pathways suggests that the CX_3CL1/CX_3CR1 axis could serve as a mechanistic link between central and peripheral alterations induced by early alcohol exposure. Dysregulation of this pathway has been associated with substance use disorders, including alcohol and cocaine, where fractalkine correlates with inflammatory and behavioral alterations (Montagud-Romero et al., 2020; Montesinos et al., 2020; García-Marchena et al., 2019). This disruption exacerbates proinflammatory responses and endothelial dysfunction, both of which are key factors in vascular injury and cardiac complications (Loh et al., 2023; Flamant et al., 2021).

To motivate our biomarker panel, we grouped outcomes into functional modules linked to fractalkine biology. Endothelial activation/adhesion markers (sE-Selectin, sICAM-1, PECAM-1, thrombomodulin) index leukocyte-endothelium crosstalk, which is amplified when inflammatory cytokines (e.g., TNFα/IFNγ) induce endothelial CX_3CL1 and signal via CX_3CR1 (Matsumiya et al., 2010; Ahn et al., 2004). Coagulation/fibrinolysis markers (PAI-1, sP-Selectin) capture the prothrombotic milieu that accompanies endothelial activation (Cesari et al., 2010). Matrix remodeling (proMMP-9) reflects extracellular-matrix turnover during vascular injury (Li et al., 2020), whereas CXCL16 provides an atheroprotective chemokine/scavenger receptor readout (Zernecke and Weber, 2010). IL13 and IL18 index type-2 and inflammasome-related inflammatory tone, respectively, which can converge with fractalkine pathways in shaping vascular and neuroimmune states (Apostolakis and Spandidos, 2013; Loh et al., 2023; Flamant et al., 2021). Because early alcohol exposure can program the HPA axis, we also included cardiac glucocorticoid (*Nr3c1*) and mineralocorticoid (*Nr3c2*) receptors to index tissue sensitivity to HPA hormones and the GR/MR balance that governs myocardial and endothelial remodeling (Carpenter et al., 2017; Lother et al., 2015). Importantly, not all analytes are direct downstream targets of CX_3CL1/CX_3CR1; rather, they represent converging vascular and immune modules that interact with fractalkine signaling and provide an integrated readout to test whether PLAE elicits a coordinated neuroimmune-vascular signature centered on, or converging with, the CX_3CL1/CX_3CR1 axis.

Based on this rationale, this study adopts a translational approach to investigate the impact of early alcohol exposure. Using a prenatal-lactational binge-like alcohol exposure model relevant to FASD, the research aims to evaluate how PLAE affects depression- and anxiety-like behaviors, stress hormone levels, and inflammatory and vascular markers in blood and heart tissue from male and female mice, including the expression of CX_3CL1 in plasma and its receptor, CX_3CR1, in cardiac tissue.

2. Materials and methods

2.1. Experimental design and timeline

This was a prenatal-lactational exposure study using a drinking-in-the-dark (DID) paradigm in breeder dams. Females were exposed to 20% (v/v) ethanol throughout gestation and lactation while single-housed. Offspring were evaluated in early adulthood on postnatal day 60 (PND60) in the elevated plus maze (EPM) and tail suspension test (TST). Trunk blood and hearts were collected at PND70 for plasma biomarker assays and cardiac gene expression (Fig. 1A).

2.2. Animals and housing

Male and female C57BL/6 inbred mice (Charles River, Barcelona, Spain) were used as breeders at the UBIOMEX animal facility within the Barcelona Biomedical Research Park (PRBB). Animals were 12 weeks old at the start of the experiment. Upon arrival, breeders were group-housed by sex (3–4 per cage) in standard individually ventilated cages under controlled environmental conditions: temperature (21 ± 1°C), humidity (55 ± 10%), and a 12-h reverse light–dark cycle (lights off from 8:00 AM to 8:00 PM). Mice acclimated for at least one week before any procedure, and all experiments were conducted during the dark

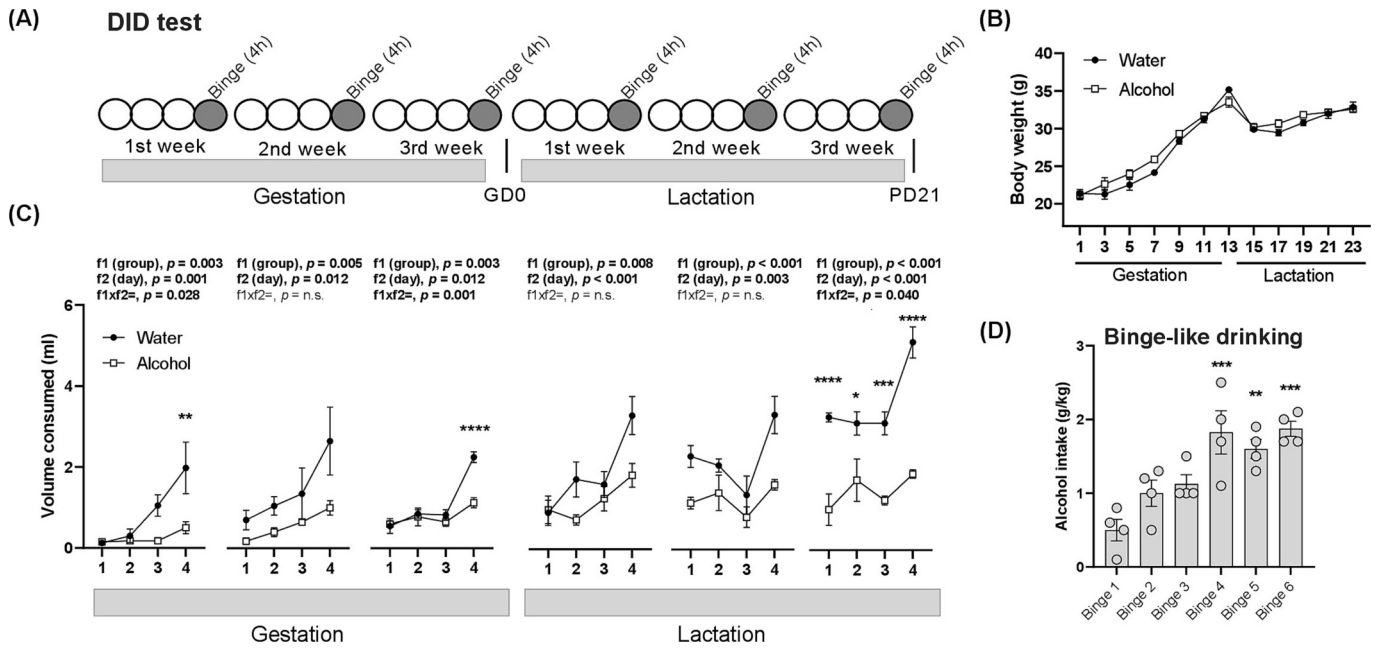

Fig. 1. Maternal DID procedure. (A) Alcohol was available 2 h/day on days 1 to 3 and 4 h on day 4 of the series during the DID procedure. (B) Maternal body weight was measured at 2-day intervals of DID test. (C) Volume of water and alcohol consumed during DID procedure throughout gestation and lactation periods. (D) Alcohol intake (g EtOH/kg) on binge days throughout DID procedure. Bars represent the mean ± SEM (4 mice/group). Data were analyzed using two-way ANOVA (B and C) and one-way ANOVA with repeated-measures (D). Sidak's test for multiple comparisons was performed: (*) denotes $p < 0.05$, (**) denotes $p < 0.01$, (***) denotes $p < 0.001$, and (****) denotes $p < 0.0001$ compared with water (C) or binge 1 (D). *P*-values in bold indicate significant main effects of factors (f1 and f2) or significant interaction (f1 × f2). Partial η^2 are reported in the text; full effect sizes (partial η2 and Cohen's *f*) are provided in Table S2.

phase under dim red lighting.

For mating, one male was paired with one female overnight. Upon detection of a copulatory plug or confirmation of pregnancy (GD0), the male was returned to group housing, and the pregnant female was immediately single-housed, where she remained throughout gestation and lactation. No males were housed with females during gestation or lactation. Pups stayed with their biological dam until weaning (PND21). After weaning, offspring were group-housed by sex (3–5 per cage) with food and water ad libitum.

2.3. Prenatal-lactational alcohol exposure in dams

Breeding mice were assigned to one of two groups: (1) alcohol-exposed (20% v/v alcohol [ethyl alcohol, Merck, Darmstadt, Germany] in tap water), or (2) water-exposed (tap water). To model binge-like intake, a 4-day DID schedule was used each week. On days 1–3, 3 h after lights-off, food was removed and the home-cage water bottle was replaced with the assigned fluid for 2 h; on day 4, access lasted 4 h (Fig. 1A). At the end of each access period, individual fluid intake was recorded, and standard food and water were restored.

Dams remained single-housed throughout gestation and lactation; male breeders were not present during DID and never exposed to alcohol. To correct for leakage/evaporation, dummy cages with identical bottles were placed on the rack each session, and drip values were subtracted from measured intakes. Fluid intake (g/kg body weight) was calculated using the 2-day average body weight; dams were weighed at 2-day intervals. This weekly 4-day DID sequence was repeated across 3 weeks of gestation and 3 weeks of lactation.

To avoid stress-related confounding during gestation and lactation, we did not perform serial blood sampling for blood alcohol concentration (BAC) in the experimental dams. In prior studies from our group using the same prenatal–lactational DID procedure (20% v/v ethanol; 2 h access on days 1–3 and 4 h on day 4 throughout gestation and lactation), maternal BAC measured immediately after the final gestational binge-like session averaged 79.27 ± 21.45 mg/dL and after the final lactational binge-like session averaged 81.57 ± 12.89 mg/dL (Cantacorps et al., 2017; Montagud-Romero et al., 2019).

Alcohol exposure was quantified as individual, drip-corrected intake (g/kg) at each DID session.

2.4. Offspring cohorts and behavioral testing

A total of 32 offspring (16 males, 16 females) were studied, divided equally between offspring of water-exposed dams and PLAE offspring. At PND60, anxiety-like behavior was assessed in the elevated plus maze (EPM) and stress-coping behavior in the tail suspension test (TST).

2.4.1. Elevated plus maze

The EPM was used to assess anxiety-like behavior following established protocols (Santin et al., 2009; Cantacorps et al., 2018). The EPM (Panlab, Barcelona, Spain) consisted of four arms (16 × 5 cm) arranged in a cross around a central square (5 × 5 cm): two closed arms (walled) and two open arms. The maze was elevated 30 cm and tested under 30 lx. Mice were placed in the central square facing an open arm and recorded for 5 min. Arm entries (all four paws inside an arm) and time in open/closed arms (as % of total) were quantified using Smart software (Panlab, Barcelona, Spain).

2.4.2. Tail suspension test

The TST was conducted to assess stress-coping behavior following specific guidelines to ensure consistency and reliability (Aslam, 2016). At PND60, mice were suspended by the tail from a horizontal bar (50 cm above the floor) using adhesive tape (17 cm strip; 2 cm attached to the tail). Each session lasted 6 min in a quiet, dimly lit room. Immobility duration (absence of voluntary movement except postural adjustments) and latency to immobility were recorded; shorter immobility was interpreted as reduced passive coping.

2.5. Sample collection

At PND70, offspring were euthanized by decapitation. Trunk blood was collected and centrifuged at 10,000 × g for 40 min at 4°C to obtain plasma. Hearts were rapidly excised; the apex was dissected, snap-frozen, and stored at − 80°C for molecular analyses.

2.6. Biochemical determinations in the plasma

Plasma samples were analyzed to determine the concentrations of corticosterone, inflammatory mediators, and cardiovascular-risk biomarkers using immunoassays. All samples were run in duplicate. For samples with absorbance below the limit of detection but above the background in the immunoassays, concentrations were set at half the minimum value interpolated from the corresponding standard curve (Whitcomb and Schisterman, 2008).

2.6.1. Corticosterone

Plasma levels of corticosterone were quantified using a solid-phase competitive enzyme-linked immunosorbent assay (ELISA), the Corticosterone Competitive ELISA Kit (Invitrogen, Thermo Fisher Scientific, Waltham, MA, USA), according to the manufacturer's instructions. Plasma samples were diluted to 1:100 using 1X Assay Buffer. Raw data were obtained at 450 nm and concentrations were expressed in pg/mL. The Corticosterone Competitive ELISA Kit exhibited a measurement range of 39 to 10,000 pg/mL with an expected limit of detection of 20.9 pg/mL. The coefficients of variation for inter-assay and intra-assay were < 8% and 6%, respectively.

2.6.2. CX_3CL1 and inflammatory mediators

Plasma levels of CX_3CL1 and other inflammatory mediators were quantified using multiplex immunoassays with the Bio-Plex Pro Mouse Chemokine Fractalkine/CX_3CL1 Set (#12002237, Bio Rad, Hercules, CA, USA) and the ProcartaPlex™ Mouse Cytokine & Chemokine Convenience Panel 1 26-Plex (#EPX260-26088–901, Thermo Fisher Scientific, Waltham, MA, USA) according to the manufacturers' instructions. Specifically, CX_3CL1 (fractalkine), GM-CSF, IFNγ, IL1β, IL2, IL4, IL5, IL6, IL12p70, IL13, IL18, and TNFα. The 96-well plates were analyzed using a Bio-Plex MAGPIX™ Multiplex Reader with Bio-Plex Manager™ MP Software (Luminex, Austin, TX, USA) and concentrations were expressed in pg/mL. Sensitivity values were as follows: CX_3CL1 (≤ 3.6 pg/mL), GM-CSF (0.19 pg/mL), IFNγ (0.09 pg/mL), IL1β (0.14 pg/mL), IL2 (0.10 pg/mL), IL4 (0.03 pg/mL), IL5 (3.2 pg/mL), IL6 (1.0 pg/mL), IL12p70 (0.21 pg/mL), IL13 (0.16 pg/mL), IL18 (9.95 pg/mL), and TNFα (0.04 pg/mL). The coefficients of variation for inter-assay and intra-assay were < 10% and < 7.5%, respectively. IL1β, IL4, and IL6 presented a high number of samples whose absorbance values were below the limit of detection but above background levels.

2.6.3. Cardiovascular markers

Plasma levels of cardiovascular disease markers were quantified using a multiplex immunoassay system with the MILLIPLEX MAP Mouse Cardiovascular Disease Magnetic Bead Panel 1 and 2 (#MCVD1/2MAG-77 K, Merck Millipore, Burlington, MA, USA) according to the manufacturer's instructions. Specifically, CXCL16, sE-Selectin, sICAM-1, PECAM-1, thrombomodulin, PAI-1, sP-Selectin, proMMP-9, troponin I (TnI), and troponin T (TnT) were quantified using a Bio-Plex MAGPIX™ Multiplex Reader with Bio-Plex Manager™ MP Software (Luminex, Austin, TX, USA). Concentrations were expressed in ng/mL. Assay sensitivities for each marker were as follows: CXCL16 (27.57 pg/mL), sE-Selectin (330 pg/mL), sICAM-1 (13.0 pg/mL), PECAM-1 (6.0 ng/mL), thrombomodulin (13.0 pg/mL), PAI-1 (0.012 ng/mL), sP-Selectin (429.0 pg/mL), proMMP-9 (8.0 pg/mL), TnI (293.0 pg/mL), and TnT (108.6 pg/mL). The coefficients of variation for inter-assay and intra-assay were < 12% and < 9%, respectively. TnI and TnT levels were not included in the study, as all samples yielded absorbance values comparable to background.

2.7. Cardiac gene expression of stress-related and inflammatory receptors

Total RNA was extracted from 25 mg heart tissue sections (the apex) using the TRIzol® method according to the manufacturer's instructions (Invitrogen, Thermo Fisher Scientific, Waltham, MA, USA). RNA samples were isolated and purified using a RNeasy MinElute Cleanup Kit (Qiagen, Hilden, Germany), including DNase I digestion, and quantified using a spectrophotometer to confirm A260/280 ratios of 1.8–2.0.

Reverse transcription was performed using 1 μg of RNA with the Transcriptor Reverse Transcriptase Kit (Roche Applied Science, Penzberg, Germany) and specific primer probe sets for *Nr3c1, Nr3c2, Cx3cr1, Tnfrsf1a, Il1r1, Tlr4*, and *Nfkbia* (**Table S1**) from TaqMan® Gene Expression Assays (Thermo Fisher Scientific, Waltham, MA, USA). Real-time qPCR was conducted using a CFX96™ Real-Time PCR Detection System (Bio-Rad, Hercules, CA, USA) with FAM dye-labeled probes from TaqMan® Gene Expression Assays. Assay specificity is ensured by probe design and manufacturer verification; no-template controls (NTCs) showed no detectable amplification. Gene expression values were normalized to *Gapdh* levels (Thermo Fisher Scientific, Waltham, MA, USA).

2.8. Statistical analysis

A priori power analysis and sample size estimation were conducted in G*Power, version 3.1 (Universität Düsseldorf, Germany) prior to study initiation for the prespecified primary outcomes in adult offspring, under a balanced 2 × 2 between-subjects design with the factors 'exposure' (PLAE vs water) and 'sex' (male vs female). Calculations targeted a two-tailed α = 0.05 and 80% power to detect effects in the moderate-to-large range (Cohen's *f*), including the 'exposure' × 'sex' interaction. Based on this planning, we aimed for n = 8 offspring per 'exposure' × 'sex' subgroup (total n = 32), consistent with ethical principles to minimize animal use while maintaining interpretability of primary endpoints. The primary outcomes were: behavioral (EPM: % time in open arms; TST: immobility duration), inflammatory/neuroimmune, vascular, and cardiac gene expression. Other measures were considered secondary or exploratory.

Data are presented as the mean ± standard error of the mean (SEM). Prior to analysis, normality was assessed using the D'Agostino–Pearson and Shapiro–Wilk tests, while Levene's test was applied to evaluate the assumption of homogeneity of variance.

One-way repeated-measures analysis of variance (ANOVA) and two-way ANOVA were conducted to compare experimental groups based on different independent variables or factors (f), such as 'group' (alcohol vs. water), 'day' (days 1, 2, 3, and 4 per week), 'exposure' (PLAE vs. water), and 'sex' (male vs. female). *Post hoc* multiple comparisons were performed using Tukey's test when the *F* statistic in one-way ANOVA with more than two factor categories or the interaction term in two-way ANOVA reached significance. Effect sizes are reported alongside *p* values: partial η2 for ANOVA main effects and interactions, and Cohen's *d* for planned pairwise comparisons. Effect sizes for all ANOVA terms are compiled in **Table S2**, which also lists the derived Cohen's *f* values. When the interaction term was non-significant, subgroup patterns were interpreted as additive main effects, and no simple-effect claims were made.

To examine associations between CX_3CL1 levels and physiological or behavioral parameters, multiple correlation analyses were conducted, and results are reported as Pearson's correlation coefficients (*r*) and corresponding *p*-values and visualized as heat maps. Because correlations were exploratory, no multiplicity correction was applied, and results are presented to generate hypotheses.

A *post hoc* sensitivity analysis, based on the achieved sample size (typically n = 7–8 per 'exposure' × 'sex' subgroup; total n = 30–32 depending on endpoint), indicated 80% power to detect large effects in

the primary outcomes, whereas smaller subgroup differences should be interpreted as exploratory. All statistical analyses were performed using GraphPad Prism, version 9 (GraphPad Software, La Jolla, CA, USA). Statistical significance was set at two-tailed $p < 0.05$.

2.9. Ethics

Every effort was made to minimize the number of animals used and to reduce their suffering. All animal care and experimental procedures were conducted in compliance with the ARRIVE guidelines (Kilkenny et al., 2010) and in accordance with the European Communities Council Directive 2010/63/EU, Regulation (EC) No. 86/609/ECC (24 November 1986), and Spanish national and regional guidelines for animal experimentation (Real Decreto 53/2013). The experimental protocols were approved by the local ethics committee (CEEA-UPF-PRBB).

3. Results

3.1. Maternal alcohol consumption during gestation and lactation

Maternal body weight was monitored throughout the DID procedure and two-way ANOVA revealed significant main effects of 'group' ($F_{1,72} = 7.612$, $p = 0.007$, partial η2 = 0.10) and 'day' ($F_{11,72} = 169.2$, $p < 0.001$, partial η2 = 0.96), with no 'group' × 'day' interaction (Fig. 1B).

The volumes of water and alcohol consumed were analyzed for each week (Fig. 1C). Two-way ANOVA revealed significant main effects of 'group' and 'day', as well as an interaction between the two factors during the first week ('group': $F_{1,24} = 11.10$, $p = 0.003$, partial η2 = 0.32; 'day': $F_{3,24} = 7.339$, $p = 0.001$, partial $\eta^2 = 0.48$; and interaction: $F_{3,24} = 3.592$, $p = 0.028$, partial η2 = 0.31), the third week ('group': $F_{1,24} = 10.96$, $p = 0.003$, partial η2 = 0.31; 'day': $F_{3,24} = 29.92$, $p < 0.001$, partial $\eta^2 = 0.79$; and interaction: $F_{3,24} = 7.203$, $p = 0.001$, partial η2 = 0.47), and the final week of the DID test, with the effects being most pronounced during the last week ('group': $F_{1,24} = 102.1$, $p < 0.001$, partial η2 = 0.81, 'day': $F_{3,24} = 8.591$, $p < 0.001$, partial $\eta^2 = 0.52$; and interaction: $F_{3,24} = 3.213$, $p = 0.040$, partial $\eta^2 = 0.29$). *Post hoc* comparisons revealed a significant increase in water consumption compared with alcohol consumption on days 4 and 12 of gestation ($p < 0.01$ and $p < 0.001$, respectively) and during the final week of lactation ($p < 0.05$).

One-way ANOVA with repeated measures for alcohol consumption revealed a significant effect of 'day' ($F_{5,18} = 9.595$, $p < 0.001$, partial $\eta^2 = 0.73$; Fig. 1D). *Post hoc* comparisons indicated significant differences in alcohol consumption on binge days 4 ($p < 0.001$), 5 ($p < 0.01$), and 6 ($p < 0.001$) compared with binge day 1.

3.2. Effects of PLAE on stress-related behaviors

To assess emotional reactivity and stress-related behaviors, offspring mice were evaluated using the EPM and the TST at PND60 with 'exposure' (f1) and 'sex' (f2) as factors (Fig. 2).

3.2.1. Locomotor activity and anxiety-like behavior

The total number of entries into the open and closed arms in the EPM, used as an index of locomotor activity, did not differ between groups: two-way ANOVA detected no main effects of 'exposure' or 'sex', and no interaction between the two factors (Fig. 2A).

In contrast, 'exposure' produced a significant main effect on the percentage of entries into the open arms ($F_{1,26} = 5.125$, $p = 0.032$, partial $\eta^2 = 0.17$; Fig. 2B), with a lower percentage in PLAE offspring.

Following the exploratory activity in the EPM, analysis of the percentage of time spent in the open arms revealed a main effect of 'exposure' ($F_{1,26} = 5.280$, $p = 0.030$, partial η2 = 0.17) and a significant 'exposure' × 'sex' interaction ($F_{1,26} = 9.858$, $p = 0.004$, partial $\eta^2 = 0.28$; Fig. 2C). *Post hoc* multiple comparisons showed female offspring from alcohol-exposed dams spent less time in the open arms than both male counterparts in the PLAE group ($p < 0.01$) and female offspring from water-exposed dams ($p < 0.01$).

3.2.2. Stress-coping behavior

In the TST, two-way ANOVA revealed a significant main effect of 'sex' on latency to immobility ($F_{1,20} = 27.73$, $p < 0.001$, partial $\eta^2 = 0.58$; Fig. 2D); female offspring displayed a longer latency than male mice. Consistently, analysis of immobility duration showed a significant main effect of 'sex' ($F_{1,20} = 8.209$, $p = 0.009$, partial $\eta^2 = 0.29$; Fig. 2E), with female mice exhibiting shorter immobility compared with males.

3.3. Neuroendocrine and immune dysregulation in offspring

We first analyzed the systemic endocrine and inflammatory profile in plasma to assess stress responsivity and immune status in the offspring. Plasma concentrations of these analytes were evaluated based on 'exposure' and 'sex'.

3.3.1. Corticosterone levels

Two-way ANOVA revealed a significant main effect of 'sex' on plasma corticosterone levels ($F_{1,26} = 13.70$, $p = 0.001$, partial $\eta^2 = 0.35$; Fig. 2F), with female offspring showing higher levels than males. No significant main effect of 'exposure' or interaction between the two factors was observed.

3.3.2. CX_3CL1 levels

Soluble CX_3CL1 levels were quantified, and two-way ANOVA revealed significant main effects of 'exposure' ($F_{1,28} = 71.31$, $p < 0.001$, partial η2 = 0.72) and 'sex' ($F_{1,28} = 17.97$, $p < 0.001$, partial η2 = 0.39), as well as a significant 'exposure' × 'sex' interaction ($F_{1,28} = 48.14$, $p < 0.001$, partial $\eta^2 = 0.63$; Fig. 3A). *Post hoc* multiple comparisons indicated that female offspring from alcohol-exposed dams (PLAE) exhibited significantly higher plasma CX_3CL1 levels compared with female offspring of water-exposed dams ($p < 0.001$) and male PLAE offspring ($p < 0.001$).

3.3.3. Inflammatory mediators

We next analyzed additional inflammatory mediators in the plasma. While several mediators were unaffected by 'exposure' or 'sex' [GM-CSF (Fig. 3B), IFNγ (Fig. 3C), IL1β (Fig. 3D), IL4 (Fig. 3F), IL6 (Fig. 3H), IL12p70 (Fig. 3I), and TNFα (Fig. 3L)], some circulating inflammatory mediators were significantly altered.

Two-way ANOVA revealed a significant 'exposure' × 'sex' interaction for plasma IL2 levels ($F_{1,27} = 5.504$, $p = 0.027$, partial $\eta^2 = 0.17$; Fig. 3E). *Post hoc* multiple comparisons indicated that female offspring from water-exposed dams exhibited significantly higher plasma IL2 levels than male offspring of water-exposed dams ($p < 0.05$).

A significant main effect of 'sex' was found for IL5 levels ($F_{1,27} = 5.501$, $p = 0.027$, partial $\eta^2 = 0.17$; Fig. 3G), with higher levels observed in female offspring compared with males.

Analysis of IL13 levels revealed significant main effects of 'exposure' ($F_{1,27} = 6.428$, $p = 0.017$, partial η2 = 0.19) and 'sex' ($F_{1,27} = 45.64$, $p < 0.001$, partial $\eta^2 = 0.63$) (Fig. 3J). Specifically, PLAE offspring exhibited significantly higher IL13 levels compared with water-exposed offspring ($p < 0.05$), and female offspring showed significantly higher levels compared with male counterparts ($p < 0.001$). In the absence of a significant interaction, this pattern is consistent with additive main effects of 'exposure' and 'sex'.

Finally, IL18 levels were significantly affected by 'exposure' ($F_{1,27} = 7.035$, $p = 0.013$, partial $\eta^2 = 0.21$; Fig. 3K), with PLAE offspring displaying significantly higher levels than offspring from water-exposed dams.

3.4. Cardiovascular-risk biomarkers and endothelial signatures

Across circulating markers related to endothelial function and

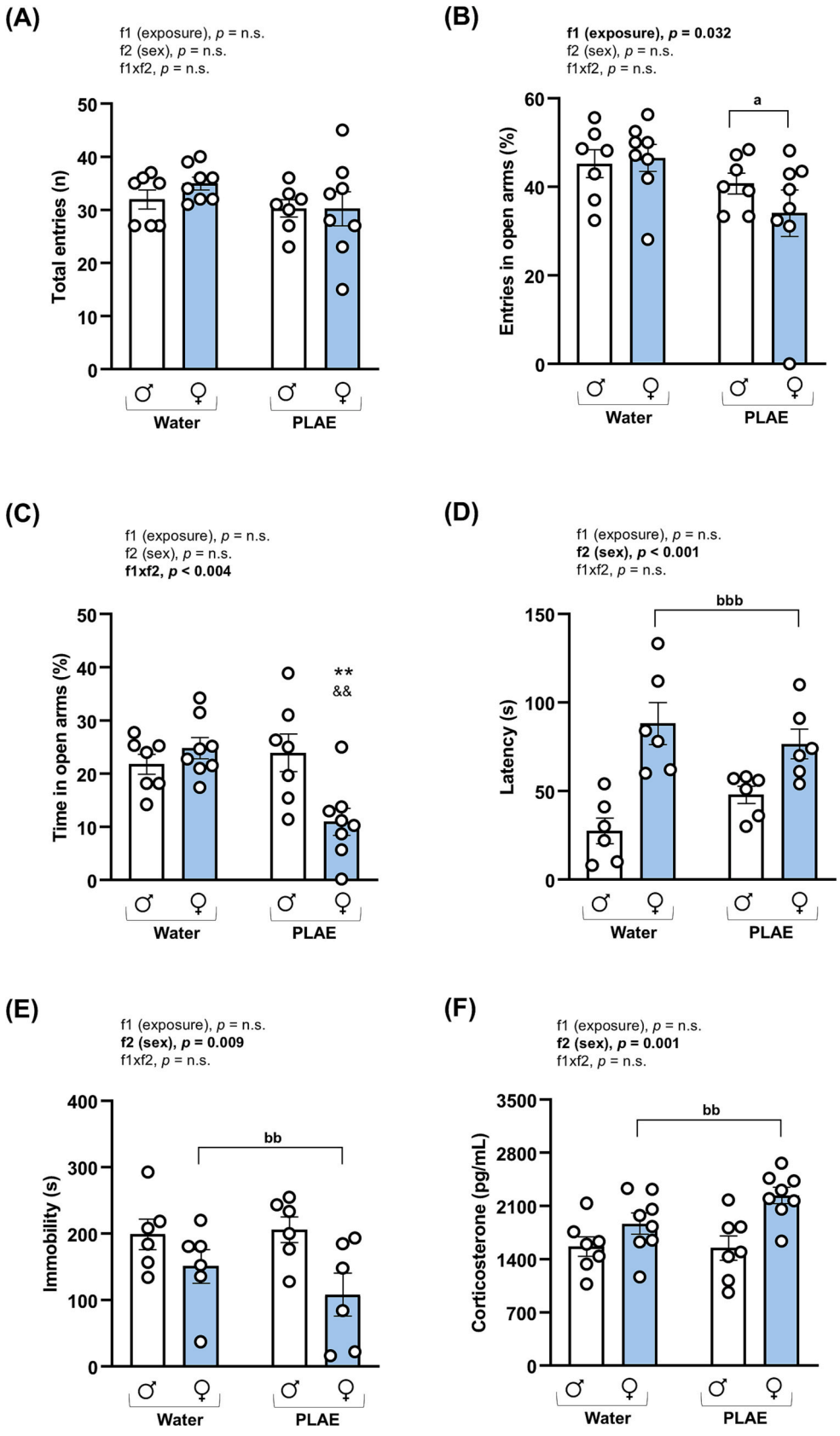

(caption on next page)

Fig. 2. Anxiety-like behavior, stress-coping behavior, and corticosterone levels in offspring exposed to PLAE. Male and female offspring mice were assessed in the EPM and TST at PND60. (A) The number of total entries in the EPM. (B) The percentage of entries in the open arms in the EPM. (C) The percentage of time spent in open arms in the EPM. (D) The latency to immobility in the TST. (E) The immobility duration in the TST. Bars represent the mean ± SEM (7–8 mice/group). Data were analyzed using a two-way ANOVA. ([a]) denotes $p < 0.05$ of 'exposure', ([bb]) denotes $p < 0.01$ of 'sex', and ([bbb]) denotes $p < 0.001$ of 'sex'. Tukey's test for multiple comparisons was performed for significant interactions: (**) denotes $p < 0.01$ compared with male offspring of water-exposed dams and ([&&]) denotes $p < 0.01$ compared with female PLAE offspring. *P*-values in bold indicate significant main effects of factors (f1 and f2) or significant interaction (f1 × f2). Partial η^2 are reported in the text; full effect sizes (partial η2 and Cohen's *f*) are provided in Table S2.

coagulation, all analytes were affected by 'exposure' and/or 'sex', with the exception of sICAM-1 (Fig. 4C).

Two-way ANOVA revealed a significant main effect of 'exposure' on plasma CXCL16 levels ($F_{1,26} = 13.57$, $p = 0.001$, partial $\eta^2 = 0.34$; Fig. 4A), with PLAE offspring showing lower levels compared with offspring of water-exposed dams.

In contrast, significant main effects of 'sex' were detected for sE-Selectin ($F_{1,26} = 14.49$, $p < 0.001$, partial $\eta^2 = 0.36$; Fig. 4B), PECAM-1 ($F_{1,26} = 5.955$, $p = 0.022$, partial $\eta^2 = 0.19$; Fig. 4D), and thrombomodulin ($F_{1,26} = 27.70$, $p < 0.001$, partial $\eta^2 = 0.52$; Fig. 4E), with female offspring exhibiting higher levels than males. Additionally, significant main effects of 'exposure' ($F_{1,26} = 8.364$, $p = 0.007$, partial $\eta^2 = 0.24$) and 'sex' ($F_{1,26} = 4.497$, $p = 0.043$, partial $\eta^2 = 0.15$) were found for plasma PAI-1 levels (Fig. 4F). Means were higher with PLAE and in females; no interaction was detected.

Plasma sP-Selectin levels were not significantly affected by either 'exposure' or 'sex'; however, a significant 'exposure' × 'sex' interaction was detected ($F_{1,26} = 5.589$, $p = 0.025$, partial $\eta^2 = 0.18$; Fig. 4G). *Post hoc* multiple comparisons indicated that male PLAE offspring exhibited significantly lower sP-Selectin levels compared with male offspring of water-exposed dams ($p < 0.05$).

Finally, analysis of proMMP-9 revealed significant main effects of 'exposure' ($F_{1,26} = 61.78$, $p < 0.001$, partial $\eta^2 = 0.70$) and 'sex' ($F_{1,26} = 9.280$, $p = 0.005$, partial $\eta^2 = 0.26$), as well as a significant 'exposure' × 'sex' interaction ($F_{1,26} = 14.43$, $p < 0.001$, partial $\eta^2 = 0.36$; Fig. 4H). *Post hoc* comparisons showed that PLAE offspring exhibited significantly higher proMMP-9 levels compared with offspring of water-exposed dams, in both males ($p < 0.001$) and females ($p < 0.05$). However, this increase was significantly less pronounced in PLAE females than in PLAE males ($p < 0.001$).

3.5. Gene expression of stress-related and inflammatory receptors in cardiac tissue

3.5.1. Nr3c1 and Nr3c2 mRNA levels

We first quantified *Nr3c1* and *Nr3c2* mRNA levels, which encode nuclear receptors involved in stress response and cardiovascular regulation. *Nr3c1* encodes the glucocorticoid receptor, activated by cortisol, while *Nr3c2* encodes the mineralocorticoid receptor, activated by aldosterone. Two-way ANOVA revealed no significant main effects of 'exposure' or 'sex', nor their interaction on *Nr3c1* gene expression (Fig. 5A). In contrast, *Nr3c2* expression analysis indicated a significant main effect of 'exposure' ($F_{1,26} = 5.336$, $p = 0.029$, partial $\eta^2 = 0.17$; Fig. 5B), with no significant main effect of 'sex' or 'exposure' × 'sex' interaction, showing higher *Nr3c2* mRNA in PLAE mice than offspring of water-exposed dams.

3.5.2. Cx3cr1 mRNA levels

Next, *Cx3cr1* mRNA levels were assessed in cardiac tissue across experimental subgroups. Two-way ANOVA revealed a significant main effect of 'exposure' ($F_{1,25} = 8.925$, $p = 0.006$, partial η2 = 0.26) and a significant 'exposure' × 'sex' interaction ($F_{1,25} = 4.683$, $p = 0.040$, partial $\eta^2 = 0.16$) (Fig. 5C). *Post hoc* multiple comparisons indicated that female PLAE offspring exhibited significantly higher *Cx3cr1* mRNA levels than female offspring of water-exposed dams and male PLAE offspring.

3.5.3. Tnfrsf1a, Il1r1, Tlr4, and Nfkbia mRNA levels

We evaluated the expression of additional inflammatory-associated genes in cardiac tissue [tumor necrosis factor receptor superfamily member 1A (*Tnfrsf1a*), interleukin-1 receptor type 1 (*Il1r1*), and toll-like receptor 4 (*Tlr4*)] to assess their potential involvement in stress-related and cardiovascular risk pathways. Two-way ANOVA revealed a significant main effect of 'exposure' on both *Tnfrsf1a* ($F_{1,26} = 4.619$, $p = 0.041$, partial $\eta^2 = 0.15$; Fig. 5D) and *Tlr4* ($F_{1,26} = 4.940$, $p = 0.035$, partial $\eta^2 = 0.16$; Fig. 5F), with elevated *Tnfrsf1a* and decreased *Tlr4* expression in PLAE offspring. No significant effect of 'exposure', 'sex', or their interaction was observed for *Il1r1* (Fig. 5E).

Finally, we examined *Nfkbia* expression, which encodes IκBα, a key regulator of the transcription factor NF-κB as inhibitor. Two-way ANOVA revealed a significant main effect of 'exposure' ($F_{1,23} = 14.03$, $p = 0.001$, partial $\eta^2 = 0.38$; Fig. 5G), with no significant main effect of 'sex' or 'exposure' × 'sex' interaction. This indicates reduced *Nfkbia* expression in PLAE offspring.

3.6. CX_3CL1 as a converging factor linking behavioral, inflammatory, and cardiovascular outcomes

We explored whether plasma CX_3CL1 levels are associated with anxiety-like behavior and behavioral despair, circulating mediators (i.e., corticosterone, inflammatory mediators, and cardiovascular-risk biomarkers), and cardiac gene-expression profiles.

3.6.1. Behavioral parameters and corticosterone

Pearson correlation analysis revealed significant associations with anxiety- and stress-related variables and corticosterone levels (Fig. 6 **A–B**). CX_3CL1 levels were inversely correlated with open-arm entries ($r_{30} = –0.382$, $p = 0.037$), time in open arms ($r_{30} = –0.677$, $p < 0.001$), and immobility duration in the TST ($r_{25} = –0.458$, $p = 0.021$). Conversely, CX_3CL1 showed a positive correlation with plasma corticosterone levels ($r_{30} = +0.683$, $p < 0.001$). These significant associations were not observed in offspring of water-exposed dams when they were separately evaluated.

3.6.2. Plasma inflammatory mediators

CX_3CL1 levels were positively associated with IL13 ($r_{31} = +0.505$, $p = 0.004$) and IL18 levels ($r_{31} = +0.431$, $p = 0.015$) (Fig. 6 **C–D**). However, no other cytokines reached significance.

3.6.3. Cardiovascular-risk biomarkers

Regarding adhesion proteins and vascular markers, CX_3CL1 levels correlated positively with CXCL16 ($r_{30} = +0.481$, $p = 0.007$) and PAI-1 levels ($r_{30} = +0.531$, $p = 0.003$) (Fig. 6 **E–F**).

3.6.4. Gene expression of stress-related and inflammatory receptors

In cardiac tissue, correlation analysis revealed a positive association between CX_3CL1 levels and mRNA expression of its cognate receptor *Cx3cr1* ($r_{30} = +0.594$, $p = 0.001$), as well as *Tnfrsf1a* ($r_{30} = +0.404$, $p = 0.027$) and *Il1r1* ($r_{30} = +0.368$, $p = 0.045$) (Fig. 6 **G–H**).

4. Discussion

The present study indicates that PLAE is associated with long-lasting, sex-specific alterations in the CX_3CL1/CX_3CR1 axis with downstream effects on neuroendocrine, inflammatory, and cardiovascular systems.

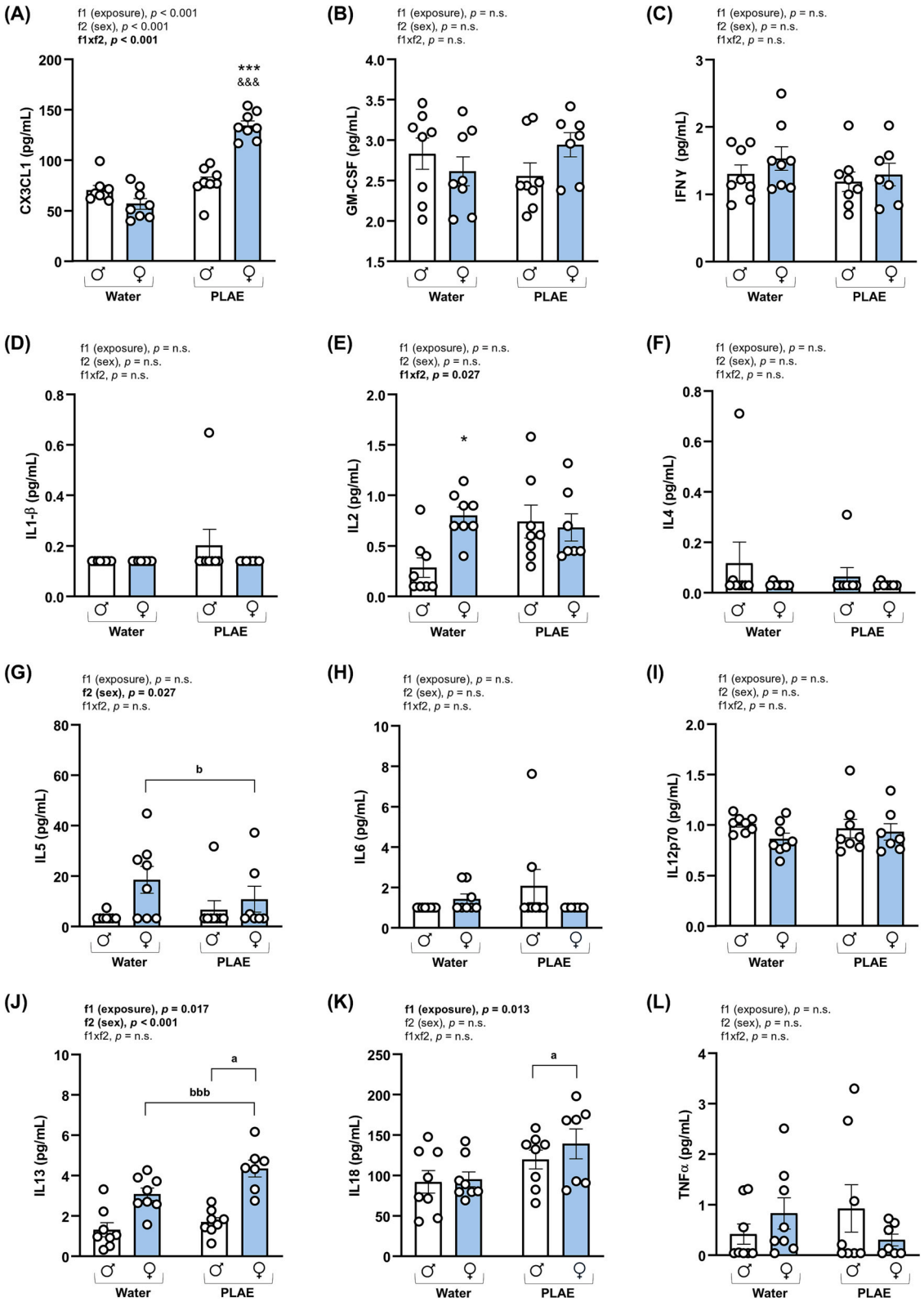

Fig. 3. Plasma levels of CX_3CL1 and other inflammatory mediators in mice exposed to PLAE. Male and female offspring mice were sacrificed at PND70 to determine these plasma analytes. (A) CX_3CL1. (B) GM-CSF. (C) IFNγ. (D) IL1β. (E) IL2. (F) IL4 (G) IL5. (H) IL6. (I) IL12p70. (J) IL13. (K) IL18. (L) TNFα. Bars represent the mean ± SEM (7–8 mice/group). Data were analyzed using a two-way ANOVA test. (^{a}) denotes $p < 0.05$ of 'exposure', (^{b}) denotes $p < 0.05$ of 'sex', and (^{bbb}) denotes $p < 0.001$ of 'sex'. Tukey's test for multiple comparisons was performed for significant interactions: (***) denotes $p < 0.001$ compared with male offspring of water-exposed dams and ($^{\&\&\&}$) denotes $p < 0.001$ compared with female PLAE offspring. *P*-values in bold indicate significant main effects of factors (f1 and f2) or significant interaction (f1 × f2). Partial η^2 are reported in the text; full effect sizes (partial η2 and Cohen's *f*) are provided in Table S2.

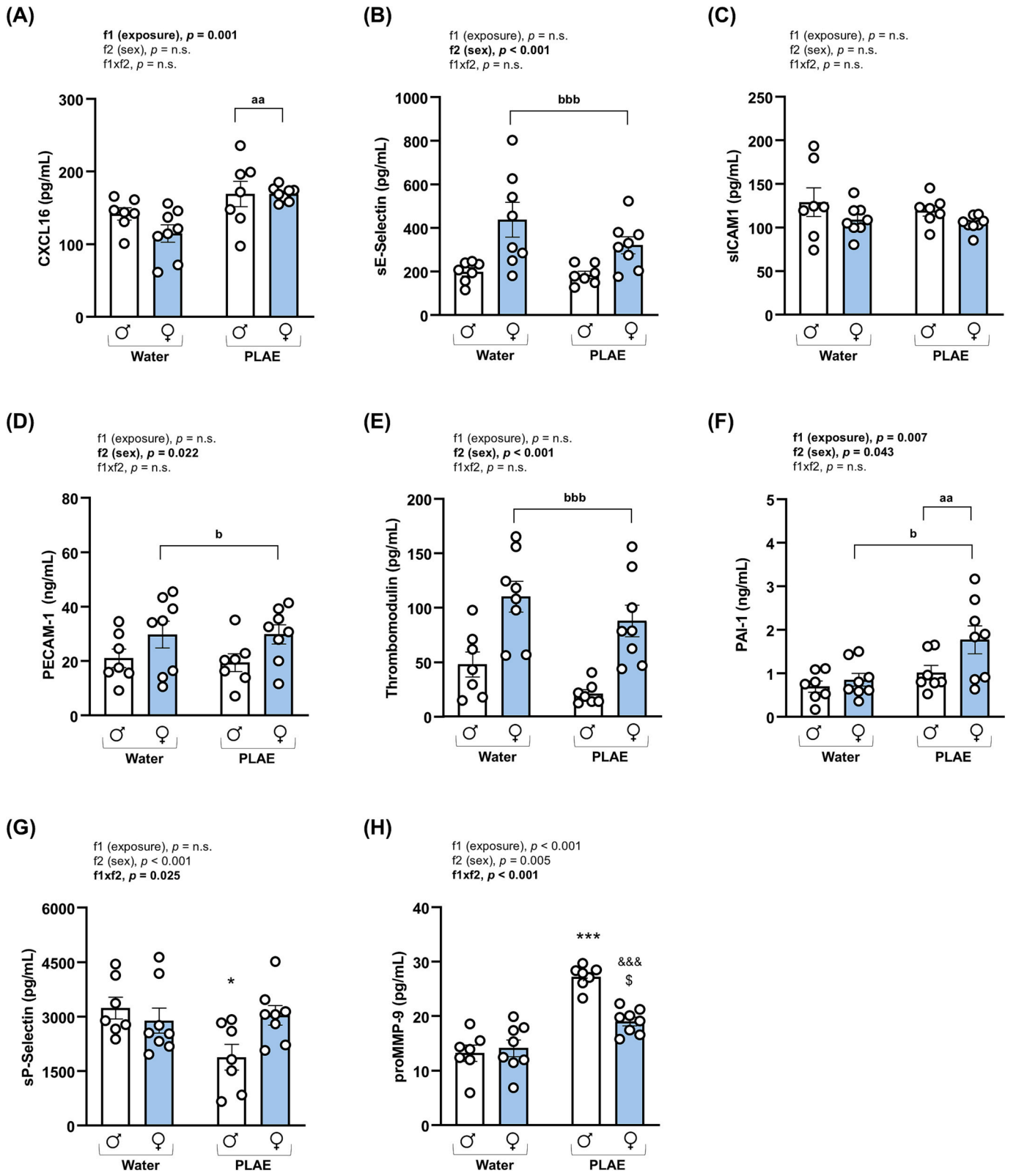

Fig. 4. Plasma levels of cardiovascular-risk markers in mice exposed to PLAE. Male and female offspring mice were sacrificed at PND70 to determine these plasma analytes. (A) CXCL16. (B) sE-Selectin. (C) sICAM1. (D) PECAM-1. (E) Thrombomodulin. (F) PAI-1. (G) sP-Selectin. (H) ProMMP-9. Bars represent the mean ± SEM (7–8 mice/group). Data were analyzed using a two-way ANOVA test. (^{aa}) denotes $p < 0.01$ of 'exposure', (^{b}) denotes $p < 0.05$ of 'sex', and (^{bbb}) denotes $p < 0.001$ of 'sex'. Tukey's test for multiple comparisons was performed for significant interactions: (*) denotes $p < 0.05$ and (***) denotes $p < 0.001$ compared with male offspring of water-exposed dams, ($^{\&\&\&}$) denotes $p < 0.001$ compared with female PLAE offspring, and ($^{\$}$) denotes $p < 0.05$ compared with female offspring of water-exposed dams. *P*-values in bold indicate significant main effects of factors (f1 and f2) or significant interaction (f1 × f2). Partial η^2 are reported in the text; full effect sizes (partial η2 and Cohen's *f*) are provided in Table S2.

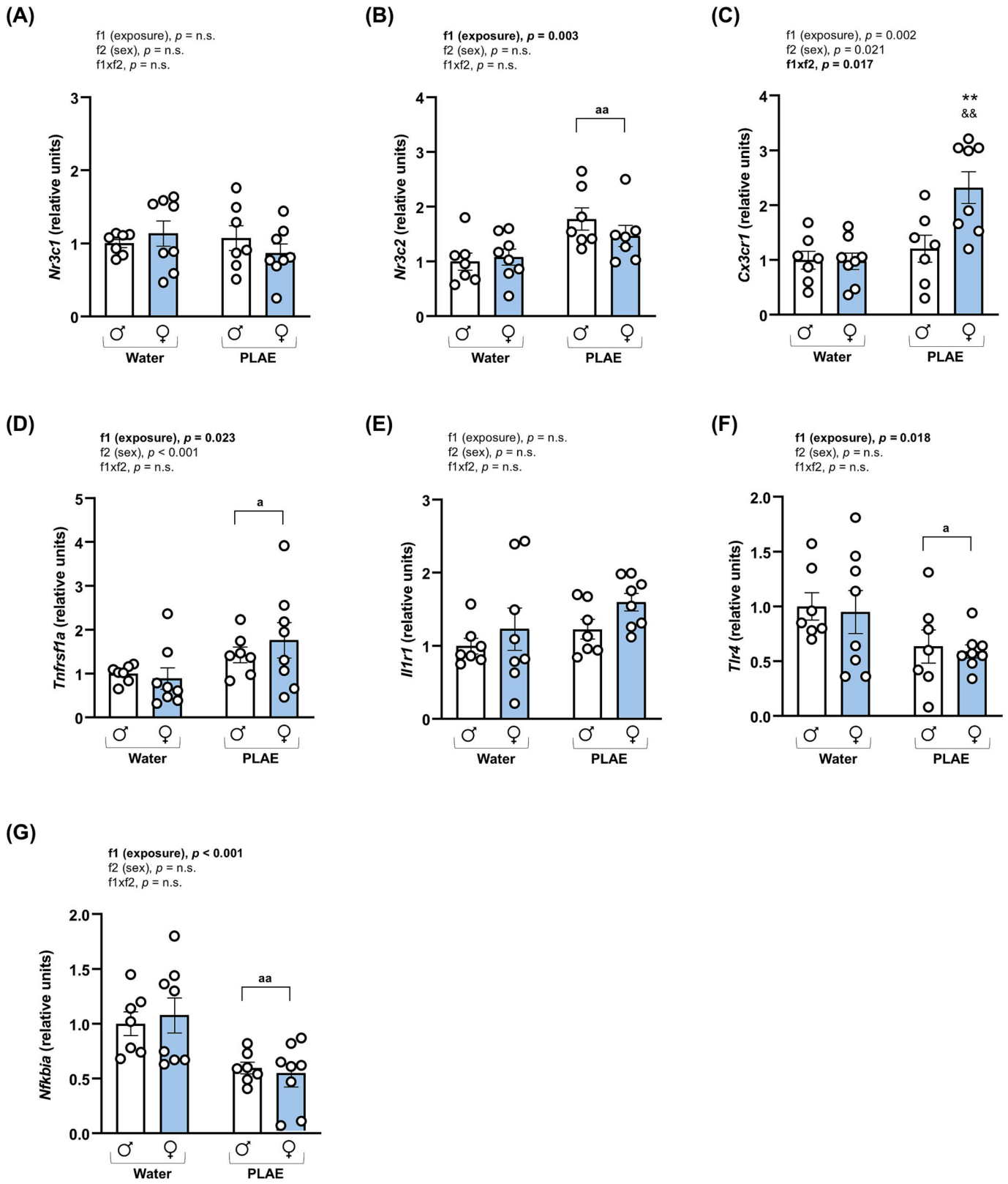

Fig. 5. Gene expression of receptors in the heart of mice exposed to PLAE. Male and female offspring mice were sacrificed at PND70 and heart was collected for these determinations. (A) *Nr3c1*. (B) *Nr3c2*. (C) *Cx3cr1*. (D) *Tnfrsf1a*. (E) *Il1r1*. (F) *Tlr4*. (G) *Nfkbia*. Bars represent the mean ± SEM (7–8 mice/group). Data were analyzed using a two-way ANOVA test. ([a]) denotes $p < 0.05$ of 'exposure' and ([aa]) denotes $p < 0.01$ of 'exposure'. Tukey's test for multiple comparisons was performed for significant interactions: (**) denotes $p < 0.01$ compared with male offspring of water-exposed dams and ([&&]) denotes $p < 0.01$ compared with female PLAE offspring. *P*-values in bold indicate significant main effects of factors (f1 and f2) or significant interaction (f1 × f2). Partial η^2 are reported in the text; full effect sizes (partial η2 and Cohen's *f*) are provided in Table S2.

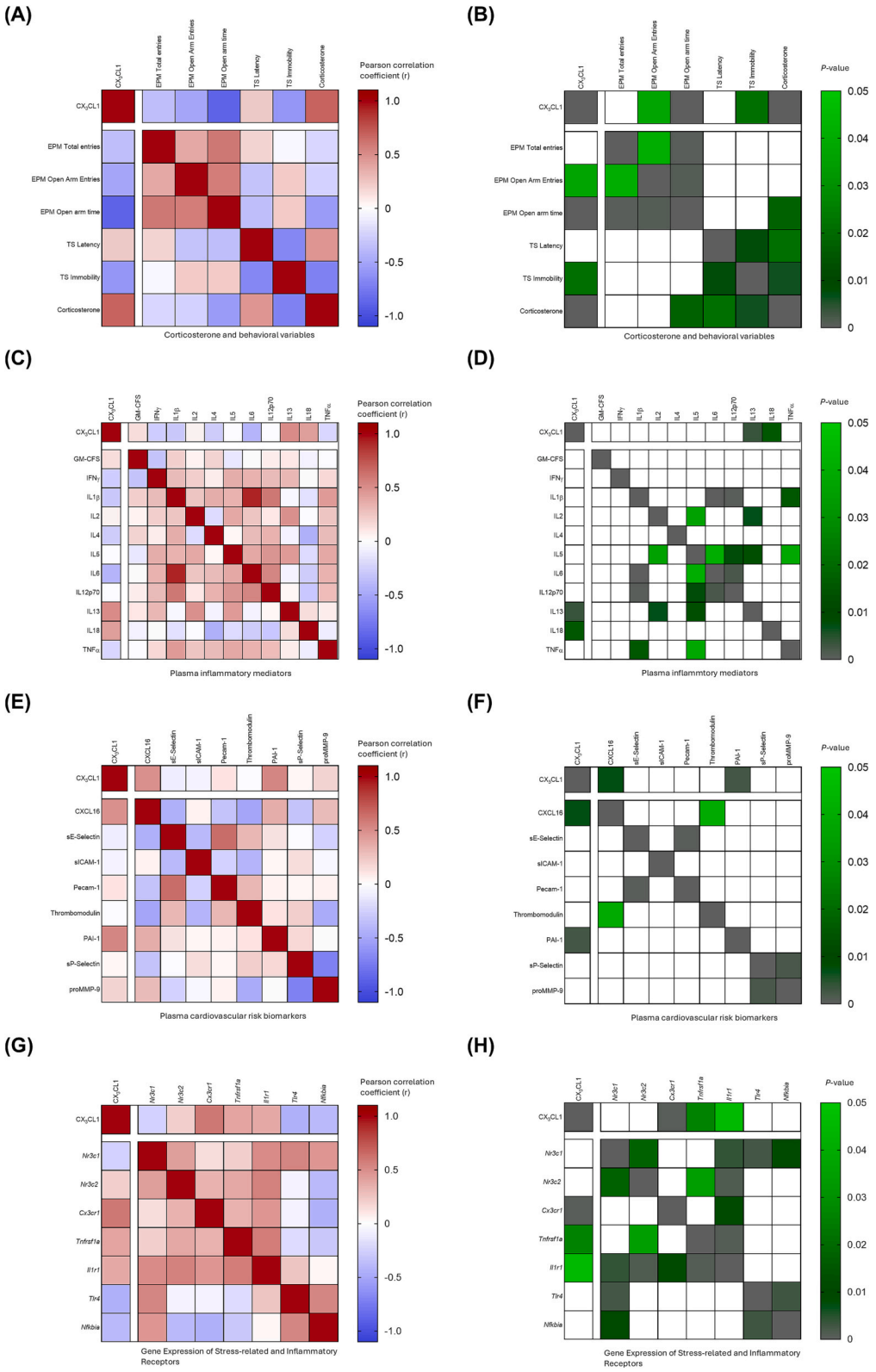

Fig. 6. Pearson correlation analysis between CX_3CL1 levels and relevant behavioral, inflammatory, and cardiovascular outcomes. (A) Pearson coefficients; and their (B) *P*-values for CX_3CL1 levels, behavioral parameters from EPM and TST, and corticosterone levels. (C) Pearson coefficients; and their (D) *P*-values for CX_3CL1 levels and other plasma inflammatory mediators. (E) Pearson coefficients; and their (F) *P*-values for CX_3CL1 levels and cardiovascular risk biomarkers. (G) Pearson coefficients; and their (H) *P*-values for CX_3CL1 levels and gene expression of stress and inflammatory receptors in cardiac tissue. Heat maps represent Pearson correlation coefficients (*r*) from –1 to 1, and significant *p*-values ($p < 0.05$). Correlations are exploratory and pooled across groups; no multiplicity correction was applied. Only significant Pearson correlations are shown.

Adult female offspring exposed to PLAE exhibited increased anxiety-like behavior, elevated plasma CX_3CL1, and upregulation of cardiac *Cx3cr1* expression, suggesting heightened fractalkine signaling. In contrast, male PLAE offspring showed no behavioral or endocrine changes but displayed increased proMMP-9 and reduced sP-Selectin, indicative of extracellular matrix remodeling. Across sexes, PLAE elevated circulating IL13, IL18, and proMMP-9, reduced CXCL16, and altered cardiac expression of *Nr3c2*, *Tnfrsf1a*, *Tlr4*, and *Nfkbia*, findings consistent with systemic inflammation and a myocardial proinflammatory set-point ('inflammatory priming'), i.e., lowered threshold for NF-κB/cytokine activation in the absence of detectable elevations in cardiac injury markers (TnI/TnT). Additionally, females as a group exhibited reduced immobility in the TST, higher plasma corticosterone, and elevated IL5, IL13, sE-Selectin, and thrombomodulin, reflecting a baseline predisposition to neuroendocrine and endothelial activation; importantly, these differences were main effects of sex without a PLAE interaction (see Fig. 3G, 3J; Fig. 4B, 4E) and are interpreted as baseline sexual dimorphism rather than outcomes attributable to PLAE or to CX_3CL1/CX_3CR1 signaling. CX_3CL1 emerged as a central biomarker, negatively correlating with exploratory and stress-coping behavior, and positively correlating with corticosterone, inflammatory and vascular biomarkers, and cardiac expression of *Cx3cr1, Tnfrsf1a*, and *Il1r1*. Because CXCL16 decreased with PLAE at the group level yet correlated positively with CX_3CL1 across individuals, we evaluated this association in the pooled sample; it should be interpreted as inter-individual covariation rather than between-group differences. Collectively, these sex-stratified associations (higher plasma CX_3CL1 with reduced open-arm exploration and higher corticosterone; positive associations with cardiac *Cx3cr1* and *Tnfrsf1a*; and covariation with PAI-1) support the hypothesis that CX_3CL1/CX_3CR1 may function as an integrative node linking behavioral, endocrine, and vascular alterations after PLAE. These data are associative and do not establish causality. Mechanistically, endothelial CX_3CL1 is robustly induced by TNFα/IFNγ, promoting leukocyte-endothelium interactions and a prothrombotic milieu (sE-Selectin, thrombomodulin, PAI-1) (Matsumiya et al., 2010; Cesari et al., 2010); concurrent elevation of proMMP-9 and reduction of CXCL16 are compatible with matrix remodeling and an atheroprone state (Li et al., 2020; Zernecke and Weber, 2010); and the positive correlations between CX_3CL1 and cardiac *Cx3cr1/Tnfrsf1a* align with known fractalkine-TNF interplay in vascular tissues (Matsumiya et al., 2010; Ahn et al., 2004).

Converging clinical and preclinical evidence indicates lasting autonomic and endothelial alterations after PLAE. Human cohorts have documented autonomic dysregulation, reduced heart-rate variability, and impaired endothelial responses in youth with prenatal alcohol exposure, and impaired vascular health has also been reported in adulthood (Kable et al., 2023). In parallel, rodent studies show persistent microglial activation and exaggerated neuroinflammatory signaling after prenatal alcohol exposure (Bake et al., 2021), providing a mechanistic framework consistent with our observation of systemic inflammatory priming. A focused review further emphasizes that vascular and neuroimmune alterations are converging contributors to FASD pathophysiology (Momin et al., 2023). With respect to fractalkine biology in addiction-related contexts, both clinical and preclinical reports implicate CX_3CL1/CX_3CR1 changes alongside inflammatory and behavioral alterations (García-Marchena et al., 2019; Araos et al., 2015; Porras-Perales et al., 2025). Together, these lines of evidence support our interpretation that the CX_3CL1/CX_3CR1 axis is a plausible converging mechanism linking neuroimmune and cardiovascular consequences of PLAE.

Consistent with clinical and preclinical indications that females are particularly vulnerable to affective sequelae of FASD (Bariselli et al., 2023; Flannigan et al., 2023), only female offspring of alcohol-exposed dams showed concurrent elevations in circulating CX_3CL1 and corticosterone, reduced open-arm exploration in the EPM, and decreased immobility in the TST. Prior work indicates that disrupting CX_3CR1 signaling heightens stress reactivity and impairs adaptive coping in mice exposed to adolescent stress and alcohol (Medina-Vera et al., 2025). Our data extend this literature by demonstrating that developmental alcohol exposure amplifies, not diminishes, CX_3CL1/CX_3CR1 signaling in females, suggesting that the directionality of fractalkine changes depends on timing, dose, and chronicity of exposure. These results align with observations of prenatal stress can reprogram the HPA axis in a sex-specific manner, increasing basal and stress-induced glucocorticoids in adult females (Carpenter et al., 2017).

Elevated soluble CX_3CL1 correlated negatively with open-arm exploration and positively with cardiac *Cx3cr1* expression. Because circulating soluble CX_3CL1 is not expected to cross an intact blood–brain barrier, we interpret plasma CX_3CL1 as a peripheral index of neuroimmune/vascular tone that covaries with anxiety-related behavior, rather than evidence that peripheral fractalkine directly drives central circuits. Within the CNS, neurons in limbic regions express CX_3CL1 and microglia express CX_3CR1, providing a plausible substrate for stress-circuit modulation (Paolicelli et al., 2014; Arnoux and Audinat, 2015). In the heart, CX_3CL1/CX_3CR1 signaling has been described as protective during early β-adrenergic stress, modulating macrophage-cardiomyocyte interactions to delay progression from hypertrophy to heart failure (Loh et al., 2023; Flamant et al., 2021). The upregulation of *Cx3cr1* observed here could thus represent a compensatory response to alcohol-induced vascular stress that becomes maladaptive over time. The concurrent increase in *Tnfrsf1a* suggests potential synergy between fractalkine and TNFα pathways, consistent with reports that inflammatory cytokines (TNFα, IFNγ, IL1) robustly induce endothelial and smooth-muscle CX_3CL1 and potentiate fractalkine-driven remodeling (Matsumiya et al., 2010; Ahn et al., 2004; Stangret et al., 2024; Raines and Ferri, 2005).

PLAE increased circulating IL13 and IL18 irrespective of sex, implicating type-2 and inflammasome-related pathways as parallel contributors to long-term risk. Elevated IL18 is a recognized predictor of future myocardial infarction and heart failure (Li et al., 2024), while IL13 promotes vascular fibrosis via TGFβ signaling (Lee et al., 2001). Concomitantly, PLAE reduced CXCL16, an atheroprotective chemokine/scavenger receptor that supports cholesterol efflux and constrains lesion growth (Zernecke and Weber, 2010). This cytokine/chemokine constellation is therefore consistent with a proatherogenic milieu well before overt disease.

The vascular biomarker profile, endothelial activation (PAI-1, thrombomodulin, sE-Selectin) and extracellular-matrix remodeling (proMMP-9), resembles early subclinical damage described in adults. PAI-1 plays a dual role by inhibiting fibrinolysis and facilitating leukocyte retention at the vascular wall (Cesari et al., 2010), whereas MMP-9 drives matrix degradation and plaque instability (Li et al., 2020). Intriguingly, these alterations were sexually dimorphic because PAI-1 predominated in females and MMP-9 in males, which aligns with clinical data that show divergent aging patterns of macro- vs. micro-vascular dysfunction across sex (DiMusto et al., 2012; Tsiknia et al., 2022). Notably, in individuals with alcohol or cocaine use disorders, endothelial adhesion molecules and proteolytic enzymes covary with cardiac injury markers, and fractalkine strongly predicts circulating troponins (Porras-Perales et al., 2025). While CX_3CL1/CX_3CR1 can be cardioprotective early on (Loh et al., 2023; Flamant et al., 2021), our data suggest that after PLAE this response may be chronically engaged and eventually maladaptive.

Cardiac upregulation of *Cx3cr1* and *Tnfrsf1a*, together with downregulation of *Tlr4* and the NF-κB inhibitor *Nfkbia*, reveals a complex rewiring in which CX_3CL1 and TNFα pathways are sensitized, while canonical TLR4 signaling is blunted. Prenatal alcohol has been reported to induce mitochondrial dysfunction and oxidative stress in cardiomyocytes (Su et al., 2024); the receptor milieu we observe may potentiate such metabolic vulnerability by lowering thresholds for inflammasome activation and TNFα–mediated apoptosis. Upregulation of *Nr3c2* (mineralocorticoid receptor) further suggests that aldosterone-driven sodium retention and fibrotic remodeling could emerge later in

life, particularly under metabolic stress (Lother et al., 2015).

Network-level studies identify fractalkine as a keystone cytokine capable of recalibrating multiple biological modules (Paolicelli et al., 2014). In this study, multivariate correlations highlighted soluble CX_3CL1 as a converging mediator across behavioral, endocrine, inflammatory, and cardiovascular domains. Elevated CX_3CL1 associated with higher corticosterone and PAI-1, reduced exploratory behavior, and enhanced cardiac *Cx3cr1* expression. Collectively, these patterns support the testable hypothesis that therapeutically targeting CX_3CL1/CX_3CR1, using approaches such as neutralizing antibodies, small-molecule antagonists, or RNA interference, may offer a dual therapeutic benefit by attenuating stress-related behavioral dysregulation and mitigating vascular injury in FASD. While these cross-domain associations are coherent with a role for CX_3CL1/CX_3CR1, the present data are associative and do not establish causality.

We propose that PLAE initiates a feed-forward loop whereby early exposure sensitizes microglia and endothelial cells to upregulate CX_3CL1. During adolescence, rising sex hormones interact with this primed neuroimmune axis, amplifying CX_3CL1/CX_3CR1 signaling and corticosterone release, particularly in females. The resultant crosstalk between the nervous and immune systems promotes anxiety-like behavior and concurrently activates cardiac macrophage-cardiomyocyte interactions, shifting the balance of endothelial proteases and inhibitors (e.g., proMMP-9 and PAI-1) toward early vascular dysfunction.

4.1. Limitations and future directions

Our sample size was powered for primary outcomes but may have missed subtler exposure × sex interactions. Measurements were restricted to early adulthood (PND60–PND70), so trajectory and durability across the lifespan remain unknown. Generalizability is limited by a single mouse strain and a specific DID exposure paradigm. We did not measure maternal BAC; therefore, intake–BAC–biomarker correlations in dams could not be established. To minimize stress-related confounds on alcohol intake, endocrine/inflammatory status, and maternal care, we prioritized limiting repeated handling and blood sampling in pregnant and lactating dams. However, in prior studies from our group using the same PLAE paradigm, maternal BACs measured immediately after the final gestational binge-like session averaged 79.27 ± 21.45 mg/dL and after the final lactational binge-like session averaged 81.57 ± 12.89 mg/dL (Cantacorps et al., 2017; Montagud-Romero et al., 2019). In addition, nursing pups showed BACs of 14.86 ± 0.82 mg/dL (PND20) and 19.38 ± 1.59 mg/dL (PND24) under the same model (Montagud-Romero et al., 2019). Alcohol intake achieved by dams in the present study was similar to that in our previous work, supporting the assumption of comparable BAC profiles. For low-abundance analytes, values near assay detection thresholds may have led to underestimation of small effects. We also lacked estrous cycle staging and deeper phenotyping (e.g., flow cytometry of CX_3CR1 + subsets, vascular reactivity, and histopathology).

Critically, the present design is associative; thus, inferences regarding the role of the CX_3CL1/CX_3CR1 pathway are correlational rather than causal. Future studies should include CNS or periphery pathway-targeted perturbations to establish causality, such as (i) pharmacological blockade or neutralization of CX_3CL1/CX_3CR1 considering peripheral-central crosstalk; (ii) genetic loss-of-function approaches (global or cell type-specific CX_3CR1 manipulation in microglia, endothelium, or cardiomyocytes, with inducible timing); and (iii) prevention and rescue paradigms testing whether pathway modulation averts or reverses behavioral, endocrine, and vascular phenotypes after PLAE. Complementary tissue-resolved mapping (single-cell/spatial transcriptomics) and functional vascular assays, together with calibration cohorts for DID intake-BAC relationships, will refine mechanism and translational relevance. Given the female-biased vulnerability observed here, defining hormonal windows of susceptibility and the efficacy of timed fractalkine-pathway modulation is a priority for future work.

4.2. Conclusions

This study supports the hypothesis that PLAE is associated with enduring, sex-specific dysregulation of the CX_3CL1/CX_3CR1 axis, with widespread effects on neuroendocrine activity, systemic inflammation, and cardiovascular homeostasis. Female PLAE offspring displayed increased anxiety-like behavior, elevated CX_3CL1 and corticosterone levels, and cardiac *Cx3cr1* upregulation, whereas male counterparts exhibited distinct vascular remodeling without behavioral or endocrine alterations. PLAE broadly disrupted inflammatory and endothelial markers and altered cardiac gene expression across sexes. Correlation analyses identified CX_3CL1 as a central integrator of behavioral, hormonal, and cardiovascular changes. These findings highlight fractalkine signaling as a potential mechanistic link between early alcohol exposure and long-term neuroimmune and cardiovascular vulnerability, supporting its consideration as a therapeutic target in FASD.

CRediT authorship contribution statement

Dina Medina-Vera: Visualization, Methodology, Investigation, Formal analysis. **Alba García-Baos:** Methodology, Investigation. **Mireia Medrano:** Methodology, Investigation. **Laura Martín-Chaves:** Methodology. **Jorge Rodríguez-Capitán:** Visualization, Formal analysis. **Fernando Rodríguez de Fonseca:** Supervision, Resources. **Antonia Serrano:** Visualization, Methodology. **Manuel Jiménez-Navarro:** Supervision, Resources. **Olga Valverde:** Writing – review & editing, Writing – original draft, Supervision, Resources, Conceptualization. **Francisco Javier Pavón-Morón:** Writing – review & editing, Writing – original draft, Supervision, Formal analysis, Conceptualization.

Declaration of competing interest

The authors declare that they have no known competing financial interests or personal relationships that could have appeared to influence the work reported in this paper.

Acknowledgements

The authors would like to thank Carolina Lobo from the Proteomics Unit of the Central Research Support Services at the University of Málaga for her technical assistance with the multiplex immunoassays. This research was supported by the following grants: Projects funded by Instituto de Salud Carlos III (ISCIII) and cofunded by the European Union (EU) and European Regional Development Fund (ERDF) (PI22/00427, PI22/01833, and PI25/02112); Project funded by Delegación de Gobierno para el Plan Nacional sobre Drogas, Ministerio de Sanidad y Consumo (PNSD 2022/020 and PNSD2023/005); Programa RICORS RIAPAD funded by ISCIII and cofunded by the EU (RD21/0009/0003); Project funded by Generalitat de Catalunya, AGAUR (2021SGR00485); Programa Fortalece funded by ISCIII, Ministerio de Ciencia, Innovación y Universidades, and cofunded by the EU (FORT23/00013); Project funded by Ministerio de Ciencia, Innovación y Universidades and Next Generation EU (PID2022-136962OB-100 - MCIN/AEI/10.13039/501100011033). DM-V and LM-C hold PFIS contracts funded by ISCIII and cofunded by the EU (FI20/00227 and FI24/00012). DM-V was also supported by an ISCIII M-AES mobility grant (MV22/00112). OV is recipient of an ICREA Academia Award (Institució Catalana de Recerca I Estudis Avançats) from the Generalitat de Catalunya. Funding for open access charge: Universidad de Málaga / CBUA.

Appendix A. Supplementary data

Supplementary data to this article can be found online at https://doi.org/10.1016/j.bbi.2026.106463.

Data availability

Data will be made available on request.

References

MacKillop, J., Agabio, R., Feldstein Ewing, S.W., Heilig, M., Kelly, J.F., Leggio, L., Lingford-Hughes, A., Palmer, A.A., Parry, C.D., Ray, L., et al., 2022. Hazardous drinking and alcohol use disorders. Nat. Rev. Dis. Primers 8. https://doi.org/10.1038/s41572-022-00406-1.

Rudenstine, S., Espinosa, A., Kumar, A., 2020. Depression and anxiety subgroups across alcohol use disorder and substance use in a National epidemiologic study. J. Dual Diagn. https://doi.org/10.1080/15504263.2020.1784498.

Howe, L.K., Fisher, L.R., Atkinson, E.A., Finn, P.R., 2021. Symptoms of anxiety, depression, and borderline personality in alcohol use disorder with and without comorbid substance use disorder. Alcohol 90. https://doi.org/10.1016/j.alcohol.2020.11.002.

Liu, Y., Yin, H., Liu, X., Zhang, L., Wu, D., Shi, Y., Chen, Y., Zhou, X., 2024. Alcohol use disorder and time perception: the mediating role of attention and working memory. Addict. Biol. 29. https://doi.org/10.1111/adb.13367.

Smith, T.S., Bryant, P.H., Fogger, S.A., 2021. Adolescent girls and alcohol use: increasing concern during the COVID-19 pandemic. J. Addict. Nurs. 32. https://doi.org/10.1097/JAN.0000000000000388.

Park, S.H., Kim, D.J., 2020. Global and regional impacts of alcohol use on public health: emphasis on alcohol policies. Clin. Mol. Hepatol. 26. https://doi.org/10.3350/cmh.2020.0160.

Oei, J.L., 2020. Alcohol use in pregnancy and its impact on the mother and child. Addiction 115. https://doi.org/10.1111/add.15036.

Almeida, L., Andreu-Fernández, V., Navarro-Tapia, E., Aras-López, R., Serra-Delgado, M., Martínez, L., García-Algar, O., Gómez-Roig, M.D., 2020. Murine models for the study of fetal alcohol spectrum disorders: an overview. Front. Pediatr. 8. https://doi.org/10.3389/fped.2020.00359.

Bariselli, S., Lovinger, D.M., 2021. Corticostriatal circuit models of cognitive impairments induced by fetal exposure to alcohol. Biol. Psychiatry 90. https://doi.org/10.1016/j.biopsych.2021.05.014.

Yang, Y., Roussotte, F., Kan, E., Sulik, K.K., Mattson, S.N., Riley, E.P., Jones, K.L., Adnams, C.M., May, P.A., O'Connor, M.J., et al., 2012. Abnormal cortical thickness alterations in fetal alcohol spectrum disorders and their relationships with facial dysmorphology. Cereb. Cortex 22. https://doi.org/10.1093/cercor/bhr193.

Cantacorps, L., Alfonso-Loeches, S., Moscoso-Castro, M., Cuitavi, J., Gracia-Rubio, I., López-Arnau, R., Escubedo, E., Guerri, C., Valverde, O., 2017. Maternal alcohol binge drinking induces persistent neuroinflammation associated with myelin damage and behavioural dysfunctions in offspring mice. Neuropharmacology 123. https://doi.org/10.1016/j.neuropharm.2017.05.034.

Gupta, K.K., Gupta, V.K., Shirasaka, T., 2016. An update on fetal alcohol syndrome—pathogenesis, risks, and treatment. Alcohol. Clin. Exp. Res. 40.

Atum, A.L.B., de Matos, L.P., de Jesus, B.C., Nasuk, G.R., da Silva, G.A., Gomes, C.P., Pesquero, J.B., Zamuner, S.R., Silva Júnior, J.A., 2023. Impact of prenatal alcohol exposure on the development and myocardium of adult mice morphometric changes, transcriptional modulation of genes related to cardiac dysfunction, and antioxidant cardioprotection. Antioxidants 12. https://doi.org/10.3390/antiox12020256.

Ninh, V.K., El Hajj, E.C., Mouton, A.J., Gardner, J.D., 2019. Prenatal alcohol exposure causes adverse cardiac extracellular matrix changes and dysfunction in neonatal mice. Cardiovasc. Toxicol. 19. https://doi.org/10.1007/s12012-018-09503-8.

Jurczyk, M., Król, M., Midro, A., Dyląg, K., Kurnik-Łucka, M., Skowron, K., Gil, K., 2024. The impact of prenatal alcohol exposure on the autonomic nervous system and cardiovascular system in rats in a sex-specific manner. Pediatr. Rep. 16, 278–287. https://doi.org/10.3390/PEDIATRIC16020024/S1.

Bake, S., Pinson, M.R., Pandey, S., Chambers, J.P., Mota, R., Fairchild, A.E., Miranda, R. C., Sohrabji, F., 2021. Prenatal alcohol-induced sex differences in immune, metabolic and neurobehavioral outcomes in adult rats. Brain Behav. Immun. 98, 86–100. https://doi.org/10.1016/j.bbi.2021.08.207.

Libby, P., 2021. Targeting inflammatory pathways in cardiovascular disease: the inflammasome, interleukin-1, interleukin-6 and beyond. Cells 10. https://doi.org/10.3390/cells10040951.

Henein, M.Y., Vancheri, S., Longo, G., Vancheri, F., 2022. The role of inflammation in cardiovascular disease. Int. J. Mol. Sci. 23. https://doi.org/10.3390/ijms232112906.

Paolicelli, R.C., Bisht, K., Tremblay, M.-Ã., 2014. Fractalkine regulation of microglial physiology and consequences on the brain and behavior. Front. Cell. Neurosci. 8. https://doi.org/10.3389/fncel.2014.00129.

Umehara, H., Bloom, E.T., Okazaki, T., Domae, N., Imai, T., 2001. Fractalkine and vascular Injury. Trends Immunol. 22, 602–607. https://doi.org/10.1016/S1471-4906(01)02051-8.

Sallusto, F., Mackay, C.R., Lanzavecchia, A., 2000. The role of chemokine receptors in primary, effector, and memory immune responses. Annu. Rev. Immunol. 18, 593–620. https://doi.org/10.1146/ANNUREV.IMMUNOL.18.1.593.

Arnoux, I., Audinat, E., 2015. Fractalkine signaling and microglia functions in the developing brain. Neural Plast. 2015. https://doi.org/10.1155/2015/689404.

Medina-Vera, D., Martín-Chaves, L., Sánchez-Marín, L., Díaz-Ottaviano, M., Gavito, A.L., Popova, O., Sánchez-Quintero, M.J., Rodríguez-Capitán, J., Rodríguez de Fonseca, F., Jiménez-Navarro, M.F., et al., 2025. Maladaptive stress-coping behavior in CX3CR1-deficient mice: impact of adolescent stress and alcohol exposure on neuroimmune responses and inflammation. Neuropharmacology 275. https://doi.org/10.1016/j.neuropharm.2025.110503.

Momin, S.Z., Le, J.T., Miranda, R.C., 2023. Vascular contributions to the neurobiological effects of prenatal alcohol exposure. Adv. Drug Alcohol Res. 3, 10924. https://doi.org/10.3389/ADAR.2023.10924/TEXT.

Apostolakis, S., Spandidos, D., 2013. Chemokines and atherosclerosis: focus on the CX3CL1/CX3CR1 pathway. Acta Pharmacol. Sin. 34. https://doi.org/10.1038/aps.2013.92.

Montagud-Romero, S., Montesinos, J., Pavón, F.J., Blanco-Gandia, M.C., Ballestín, R., Rodríguez de Fonseca, F., Miñarro, J., Guerri, C., Rodríguez-Arias, M., 2020. Social Defeat-induced increase in the conditioned rewarding effects of cocaine: role of CX3CL1. Prog. Neuropsychopharmacol. Biol. Psychiatry 96. https://doi.org/10.1016/j.pnpbp.2019.109753.

Montesinos, J., Castilla-Ortega, E., Sánchez-Marín, L., Montagud-Romero, S., Araos, P., Pedraz, M., Porras-Perales, Ó., García-Marchena, N., Serrano, A., Suárez, J., et al., 2020. Cocaine-induced changes in CX3CL1 and inflammatory signaling pathways in the hippocampus: association with IL1β. Neuropharmacology 162. https://doi.org/10.1016/j.neuropharm.2019.107840.

García-Marchena, N., Barrera, M., Mestre-Pintó, J.I., Araos, P., Serrano, A., Pérez-Mañá, C., Papaseit, E., Fonseca, F., Ruiz, J.J., De Fonseca, F.R., et al., 2019. Inflammatory mediators and dual depression: potential biomarkers in plasma of primary and substance-induced major depression in cocaine and alcohol use disorders. PLoS One 14, e0213791. https://doi.org/10.1371/JOURNAL.PONE.0213791.

Loh, S.X., Ekinci, Y., Spray, L., Jeyalan, V., Olin, T., Richardson, G., Austin, D., Alkhalil, M., Spyridopoulos, I., 2023. Fractalkine signalling (CX3CL1/CX3CR1 Axis) as an emerging target in coronary artery disease, J. Clin. Med., 12, 4821, doi:10.3390/JCM12144821.

Flamant, M., Mougenot, N., Balse, E., Le Fèvre, L., Atassi, F., Gautier, E.L., Le Goff, W., Keck, M., Nadaud, S., Combadière, C., et al., 2021. Early activation of the cardiac CX3CL1/CX3CR1 axis delays β-adrenergic-induced heart failure. Sci. Rep. 11, 17982. https://doi.org/10.1038/s41598-021-97493-z.

Matsumiya, T., Ota, K., Imaizumi, T., Yoshida, H., Kimura, H., Satoh, K., 2010. Characterization of synergistic induction of CX3CL1/fractalkine by TNF-alpha and IFN-gamma in vascular endothelial cells: an essential role for TNF-alpha in post-transcriptional regulation of CX3CL1. J. Immunol. 184, 4205–4214. https://doi.org/10.4049/JIMMUNOL.0903212.

Ahn, S.Y., Cho, C.H., Park, K.G., Lee, H.J., Lee, S., Park, S.K., Lee, I.K., Koh, G.Y., 2004. Tumor necrosis factor-α induces fractalkine expression preferentially in arterial endothelial cells and mithramycin A suppresses TNF-α-induced fractalkine expression. Am. J. Pathol. 164, 1663–1672. https://doi.org/10.1016/S0002-9440(10)63725-X.

Cesari, M., Pahor, M., Incalzi, R.A., 2010. Review: plasminogen activator inhibitor-1 (PAI-1): a key factor linking fibrinolysis and age-related subclinical and clinical conditions. Cardiovasc. Ther. 28. https://doi.org/10.1111/j.1755-5922.2010.00171.x.

Li, T., Li, X., Feng, Y., Dong, G., Wang, Y., Yang, J., 2020. The role of matrix metalloproteinase-9 in atherosclerotic plaque instability. Mediators Inflamm. 2020, 1–13. https://doi.org/10.1155/2020/3872367.

Zernecke, A., Weber, C., 2010. Chemokines in the vascular inflammatory response of atherosclerosis. Cardiovasc. Res. 86, 192–201. https://doi.org/10.1093/cvr/cvp391.

Carpenter, T., Grecian, S.M., Reynolds, R.M., 2017. Sex differences in early-life programming of the hypothalamic–pituitary–adrenal axis in humans suggest increased vulnerability in females: a systematic review. J. Dev. Orig. Health Dis. 8, 244–255. https://doi.org/10.1017/S204017441600074X.

Lother, A., Moser, M., Bode, C., Feldman, R.D., Hein, L., 2015. Mineralocorticoids in the heart and vasculature: new insights for old hormones. Annu. Rev. Pharmacol. Toxicol. 55, 289–312. https://doi.org/10.1146/annurev-pharmtox-010814-124302.

Cantacorps, L., Alfonso-Loeches, S., Moscoso-Castro, M., Cuitavi, J., Gracia-Rubio, I., López-Arnau, R., Escubedo, E., Guerri, C., Valverde, O., 2017. Maternal alcohol binge drinking induces persistent neuroinflammation associated with myelin damage and behavioural dysfunctions in offspring mice. Neuropharmacology 123, 368–384. https://doi.org/10.1016/j.neuropharm.2017.05.034.

Montagud-Romero, S., Cantacorps, L., Valverde, O., 2019. Histone deacetylases inhibitor trichostatin a reverses anxiety-like symptoms and memory impairments induced by maternal binge alcohol drinking in mice. J. Psychopharmacol. 33, 1573–1587. https://doi.org/10.1177/0269881119857208.

Santin, L.J., Bilbao, A., Pedraza, C., Matas-Rico, E., López-Barroso, D., Castilla-Ortega, E., Sánchez-López, J., Riquelme, R., Varela-Nieto, I., De La Villa, P., et al., 2009. Behavioral phenotype of MaLPA1-null mice: increased anxiety-like behavior and spatial memory deficits. Genes Brain Behav. 8. https://doi.org/10.1111/j.1601-183X.2009.00524.x.

Cantacorps, L., González-Pardo, H., Arias, J.L., Valverde, O., Conejo, N.M., 2018. Altered brain functional connectivity and behaviour in a mouse model of maternal alcohol binge-drinking. Prog. Neuropsychopharmacol. Biol. Psychiatry 84, 237–249. https://doi.org/10.1016/j.pnpbp.2018.03.006.

Aslam, M., 2016. Tail suspension test to evaluate the antidepressant activity of experimental drugs. Bangladesh J. Pharmacol. 11. https://doi.org/10.3329/bjp.v11i2.26517.

Whitcomb, B.W., Schisterman, E.F., 2008. Assays with lower detection limits: implications for epidemiological investigations. Paediatr. Perinat. Epidemiol. 22. https://doi.org/10.1111/j.1365-3016.2008.00969.x.

Kilkenny, C., Browne, W.J., Cuthill, I.C., Emerson, M., Altman, D.G., 2010. Improving bioscience research reporting: the arrive guidelines for reporting animal research. PLoS Biol. https://doi.org/10.1371/journal.pbio.1000412.

Kable, J.A., Mehta, P.K., Rashid, F., Coles, C.D., 2023. Path analysis of the impact of prenatal alcohol on adult vascular function. Alcohol: Clin. Experim. Res. 47, 116–126. https://doi.org/10.1111/ACER.14970.

Araos, P., Pedraz, M., Serrano, A., Lucena, M., Barrios, V., García-Marchena, N., Campos-Cloute, R., Ruiz, J.J., Romero, P., Suárez, J., et al., 2015. Plasma profile of pro-inflammatory cytokines and chemokines in cocaine users under outpatient treatment: influence of cocaine symptom severity and psychiatric co-morbidity. Addict. Biol. 20, 756–772. https://doi.org/10.1111/ADB.12156.

Porras-Perales, Ó., Segovia-Reyes, J., Crespo-Delgado, Á., Ruiz-González, D., Flores-López, M., Medina-Vera, D., Sánchez-Marín, L., Martín-Chaves, L., Requena-Ocaña, N., Molina-Ramos, A.I., et al., 2025. Distinct cardiac troponin alterations in patients with cocaine and alcohol use disorders during abstinence for cardiovascular risk assessment. Sci. Rep. 15, 21887. https://doi.org/10.1038/s41598-025-08041-y.

Bariselli, S., Reuveni, N., Westcott, N., Mateo, Y., Lovinger, D.M., 2023. Postnatal ethanol exposure impairs social behavior and operant extinction in the adult female mouse offspring. Front. Neurosci. 17, doi:10.3389/fnins.2023.1160185.

Flannigan, K., Poole, N., Cook, J., Unsworth, K., 2023. Sex-related differences among individuals assessed for fetal alcohol spectrum disorder in Canada. Alcohol: Clin. Experim. Res. 47, 613–623. https://doi.org/10.1111/acer.15017.

Stangret, A., Sadowski, K.A., Jabłoński, K., Kochman, J., Opolski, G., Grabowski, M., Tomaniak, M., 2024. Chemokine fractalkine and non-obstructive coronary artery disease—is there a link? Int. J. Mol. Sci., 25, 3885, doi:10.3390/IJMS25073885.

Raines, E.W., Ferri, N., 2005. Thematic review series: the immune system and atherogenesis. cytokines affecting endothelial and smooth muscle cells in vascular disease. J. Lipid Res. 46, 1081–1092. https://doi.org/10.1194/jlr.r500004-jlr200.

Li, F., Zhang, Y., Wang, Y., Cai, X., Fan, X., 2024. Cytokine gene variants as predisposing factors for the development and progression of coronary artery disease: a systematic review. Biomolecules 14, 1631. https://doi.org/10.3390/biom14121631.

Lee, C.G., Homer, R.J., Zhu, Z., Lanone, S., Wang, X., Koteliansky, V., Shipley, J.M., Gotwals, P., Noble, P., Chen, Q., et al., 2001. Interleukin-13 induces tissue fibrosis by selectively stimulating and activating transforming growth factor B1. J. Exp. Med. 194, 809–822. https://doi.org/10.1084/jem.194.6.809.

DiMusto, P.D., Lu, G., Ghosh, A., Roelofs, K.J., Su, G., Zhao, Y., Lau, C.L., Sadiq, O., McEvoy, B., Laser, A., et al., 2012. Increased PAI-1 in females compared with males is protective for abdominal aortic aneurysm formation in a rodent model. Am. J. Physiol.-Heart Circul. Physiol. 302, H1378–H1386. https://doi.org/10.1152/ajpheart.00620.2011.

Tsiknia, A.A., Sundermann, E.E., Reas, E.T., Edland, S.D., Brewer, J.B., Galasko, D., Banks, S.J., 2022. Sex differences in Alzheimer's disease: plasma MMP-9 and markers of disease severity. Alzheimers Res. Ther. 14, 160. https://doi.org/10.1186/s13195-022-01106-4.

Su, Y., Yu, Y., Quan, J., Zhang, J., Xu, Y., 2024. Alcohol exposure during pregnancy induces cardiac mitochondrial damage in offspring mice. Birth Defects Res. 116, doi:10.1002/bdr2.2369.